JACS
JOURNAL OF THE AMERICAN CHEMICAL SOCIETY

Article

pubs.acs.org/JACS

Reversible Near-Infrared Fluorescent Probe Introducing Tellurium to Mimetic Glutathione Peroxidase for Monitoring the Redox Cycles between Peroxynitrite and Glutathione in Vivo

Fabiao Yu, Peng Li, Bingshuai Wang, and Keli Han*

State Key Laboratory of Moleclar Reaction Dynamics, Dalian Institute of Chemical Physics, Chinese Academy of Sciences, 457 Zhongshan Road, Dalian, China 116023

Supporting Information

ABSTRACT: The redox homeostasis between peroxynitrite and glutathione is closely associated with the physiological and pathological processes, e.g. vascular tissue prolonged relaxation and smooth muscle preparations, attenuation hepatic necrosis, and activation matrix metalloproteinase-2. We report a near-infrared fluorescent probe based on heptamethine cyanine, which integrates with telluroenzyme mimics for monitoring the changes of $ONOO^-$/GSH levels in cells and in vivo. The probe can reversibly respond to $ONOO^-$ and GSH and exhibits high selectivity, sensitivity, and mitochondrial target. It is successfully applied to visualize the changes of redox cycles during the outbreak of $ONOO^-$ and the antioxidant GSH repair in cells and animal. The probe would provide a significant advance on the redox events involved in the cellular redox regulation.

INTRODUCTION

Endogenous peroxynitrite ($ONOO^-$) has been recognized as a strong oxidant agent in vivo. This chemical property of peroxynitrite makes it a central biological pathogenic factor in a variety of diseases, such as cardiovascular, neurodegenerative, and inflammatory disorders.[1] Peroxynitrite has also shown as a nitrating agent causing nitrative stress in cells, but more investigations on endogenous $ONOO^-$ have been devoted to modulate signal transduction pathways via its ability to nitrate biomolecules including nitrated tyrosine residues, 8-nitroguanosine, and nitro fatty acids and thereby influencing cellular processes.[2] Peroxynitrite can also be as a potential candidate for anticancer drugs.[3] Intracellular peroxynitrite is produced by the diffusion-controlled reaction of nitric oxide (NO) and superoxide ($O_2^{\bullet -}$) radicals at rate of $\sim 10^{10}$ M^{-1} s^{-1}.[3] The endogenous abnormally high concentration of peroxynitrite has been estimated up to 100 μM per min in immune system cells (notably in macrophages) when against invading microorganisms (e.g., Chagas' disease and bacterial infection),[4] whereas the steady-state concentration of peroxynitrite is assessed to be in the nanomolar scale range for hours' time.[5] To provide interpretation for these paradoxes that mentioned above, we consider the intracellular redox homeostasis between peroxynitrite and endogenous antioxidants. Cells employ the expression of $ONOO^-$-specific scavengers glutathione peroxidase (GPx, a selenoenzyme), to maintain the concentration of $ONOO^-$ below a toxic threshold. However, many recent efforts are focused on the GPx-like telluroenzyme mimics to explore how peroxynitrite acts in physiological and pathological processes. Small artificial organic molecule probes have emerged as one of the most powerful biotechniques to detect physiologically active species in living system with high temporal and spatial resolution.[6] Not only can they prove useful in the detection of disease states but also they will allow for a screening-type analysis of potential signal transduction pathways in cells. As known, intracellular $ONOO^-$ redox homeostasis is a complex redox process in living systems. The process includes signal transduction, homeostasis regulation, and oxidative stress and antioxidant repair in time in living cells. Therefore, we strive to develop a probe that can respond reversibly to the changes in the redox homeostasis regulation via a redox-based mechanism for visualizing states of this redox cycles.

Intracellular thiols provide abundant reducing sources that are central to cellular redox homeostasis in the antioxidant defense systems. Among these biothiols, glutathione (GSH) is the most abundant endogenous thiol, whose concentration ranges from 1 to 15 mM depending on the cell types.[7] GSH manipulates the redox homeostasis through the equilibrium between the reduced form (GSH) and disulfides form (GSSG).[8] Especially in mitochondria, the primary site of formation and reactions of intracellular peroxynitrite,[1,9] GSH exists predominantly in the reduced form involved a GSH/GSSG molar ratio of >100:1.[8,10] $ONOO^-$ can significantly perturb the mitochondrial GSH/GSSG ratio and further take the responsibility for the irreversible damage to respiration. Interpreting the regulation and interplay between peroxynitrite and GSH also can reveal the physiological and pathological roles of endogenous peroxynitrite. In order to distinct the roles of $ONOO^-$, it is very crucial to establish a real-time visualization method for monitoring the redox homeostasis changes between peroxynitrite and glutathione in vivo.

Received: February 11, 2013
Published: April 27, 2013

dx.doi.org/10.1021/ja401360a | J. Am. Chem. Soc. 2013, 135, 7674−7680

After confirming the key point of our research, we design and synthesize a single fluorescent probe Cy-NTe for the reversible detection of $ONOO^-$ and GSH (Scheme 1). The organic small molecule fluorescent probe Cy-NTe features a telluroenzyme (NTe) fluorescent modulator that is integrated into heptamethine cyanine platform (Cy). The probe is found to be selective for the reversible monitoring of $ONOO^-$ and GSH redox cycles with a detection limit of 9.17×10^{-7} M in potassium phosphate solution. The fluorescent response of Cy-NTe to $ONOO^-$ and GSH could complete within 10 and 5 min, respectively. These features play a crucial role in the redox cycle detection on account of the fast metabolism in homeostasis regulation.

Scheme 1. Proposed Reaction Mechanism, Structures of Cy-NTe and Its Oxidized Product Cy-NTeO

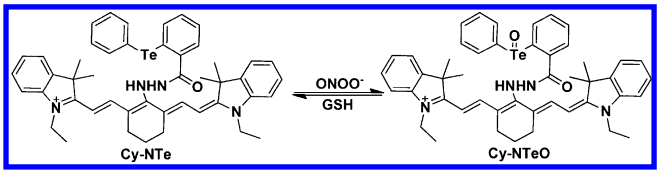

RESULTS AND DISCUSSION

Design and Synthesis of Fluorescent Probe Cy-NTe. Conceiving sensitive and selective fluorescent probes for peroxynitrite is of critical importance for understanding its roles in disease and signal transduction. To date, some fluorescent probes for $ONOO^-$ detection have been reported but can only respond irreversibly to a single initial detection event.[11] In contrast, small molecule probes that can respond reversibly to changes in redox homeostasis regulation would be much more valuable for visualizing cycles of redox signaling, stress, repair, and their dynamic interconversion.[12] Only a few redox-sensitive reversible fluorescence probes for redox stress have been developed.[12,13] Additionally, the fluorescence excitation and emission of the reported probes most locate in the UV or visible region, which can cause interference from biological autofluorescence. Therefore, it is necessary to develop a reversible fluorescent probe that has near-infrared (NIR) absorption and emission for peroxynitrite detection in vivo. Recently, our group has focused on the development of a selenium-containing reversible fluorescent probe for monitoring cellular redox changes.[14] Our overall strategy for imaging the redox cycle in live biological systems is inspired by exploiting a mimic of selenoenzyme, GPx, as redox reservoirs in cells.[15] It is reported that the GPx-like activity of telluroenzyme analogue displays much higher activity than the organoselenium analogue.[16] Next, we selected 2-(phenyltellanyl)benzohydrazide (NTe) as fluorescent modulator because the organotellurium analogue undergone a reversible spirocyclization, which could protect the telluroenzyme mimics moiety from overoxidation by $ONOO^-$.[17] We chose heptamethine cyanine (Cy) as a signal transducer because this fluorophore platform possessed near-infrared (NIR) absorption and emission profiles to maximize tissue penetration while minimizing the absorbance of heme in hemoglobin and myoglobin, water, and lipids.[18] Our design strategy to the fluorescent probe for intracellular $ONOO^-$/GSH redox cycles was illustrated in Scheme 1. We reasoned that the detection mechanism relied on a fast photoinduced electron transfer (PET) process.[14,18b,19] Scheme 2 summarized the synthesis of Cy-NTe from the appropriately fluorophore Cy.7.Cl and receptor NTe. The optimization of diphenyl ditelluride (**2**) started from readily available bromobenzene and tellurium;[20] 2-(methoxycarbonyl) benzenediazonium tetrafluoroborate (**3**) was steadily prepared as an isolable arenediazonium salt.[7a] Our pivotal material was methyl 2-(phenyltellanyl)-benzoate (**4**), which followed a nucleophilic aromatic addition–elimination reaction with release of N_2.[21] Reaction of hydrazine hydrate with **4** gave 2-(phenyltellanyl)benzohydrazide (**5**) smoothly. Treatment of **5** with fluorophore Cy.7.Cl in anhydrous acetonitrile resulted in the formation of our probe Cy-NTe.[22] The synthetic details of these compounds were shown in the Supporting Information.

Scheme 2. Strategy and Synthesis of Probe Cy-NTe[a]

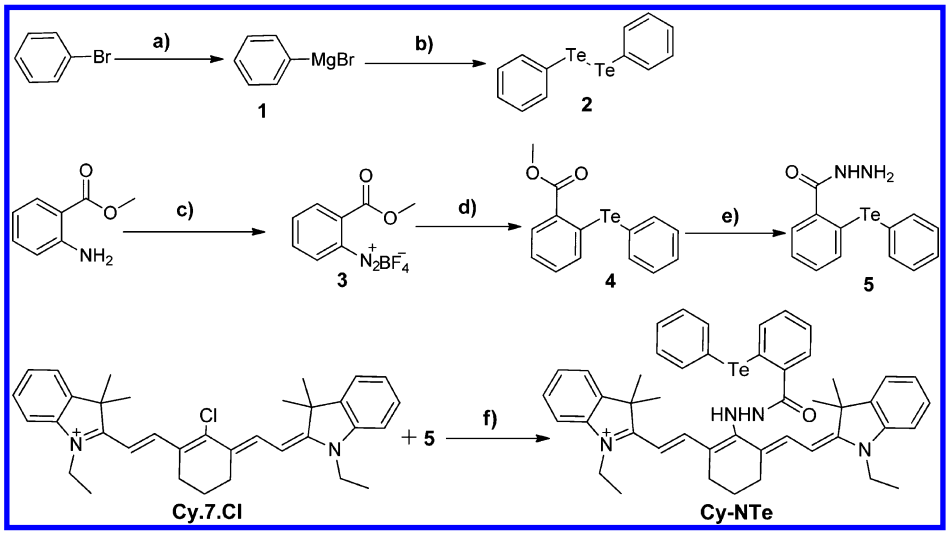

[a]Notes: (a) Mg, anhydrous THF, reflux 2 h; (b) phenylmagnesium bromide (**1**) was added into suspension of Te, anhydrous THF, reflux 4 h, after added saturated NH_4Cl, bubbled air 12 h; (c) $BF_3{\cdot}Et_2O$, isoamyl nitrite, anhydrous CH_2Cl_2, −15 °C, 1 h; (d) diphenyl ditelluride (**2**), Zn, dimethyl carbonate, 85 °C, 12 h; (e) 85% hydrazine hydrate, ethanol, reflux 24 h; (f) 2-(phenyltellanyl)benzohydrazide (**5**), anhydrous acetonitrile, 50 °C, 12 h.

dx.doi.org/10.1021/ja401360a | J. Am. Chem. Soc. 2013, 135, 7674–7680

Investigation of Spectral Properties of Probe Cy-NTe. We examined the spectral properties of our probe Cy-NTe under simulated physiological conditions (50 mM PBS pH 7.4, 10 μM). The probe exhibits λ_{max} of absorption and emission at 793 nm ($\varepsilon_{793\ nm}$ = 95 390 M^{-1} cm^{-1}) and 820 nm respectively in the NIR window. In response to $ONOO^-$, Cy-NTe shows an increase in fluorescence intensity (part b of Figure 1)

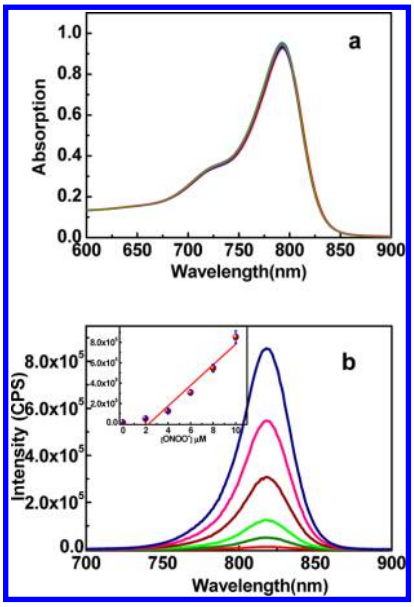

Figure 1. Absorption (a) and fluorescence emission (b) spectral changes of Cy-NTe (10 μM) after 10 min upon addition of 0, 2, 4, 6, 8, 10 μM peroxynitrite. Spectra were acquired in 50 mM PBS (pH 7.4, acetonitrile 10% v/v) with excitation at 793 nm and emission colleting window from 700 to 900 nm. Inset: Fluorescence intensities at 820 nm response to peroxynitrite concentration.

corresponding to a quantum yield increase from Φ = 0.0032 for the apo dye Cy-NTe to Φ = 0.0431 for the peroxynitrite oxidized probe Cy-NTeO. During the off–on fluorescence processes, the absorbance spectra have no significant change (part a of Figure 1). To evaluate the ability of Cy-NTe in the determination of $ONOO^-$ concentration under simulated physiological conditions, the probe is treated with $ONOO^-$ under various concentrations (0 to 10 μM). The fluorescence intensity at 820 nm was linearly proportional to the $ONOO^-$ concentration in the given range (inset in part b of Figure 1, r = 0.963) indicating the suitability of Cy-NTe for quantitative and qualitative detection of $ONOO^-$ potentially. The detection limit was determined to be 9.17 × 10^{-7} M under the experimental conditions.

Selectivity of Cy-NTe toward Peroxynitrite in Solution and in Living Cells. The specificity of Cy-NTe toward $ONOO^-$ was verified. The probe was tested against physiological relevant reactive oxygen and nitrogen species in solution and in living cells. The fluorescence response of Cy-NTe was found to be good selective to $ONOO^-$ over other biologically relevant reactive oxygen and nitrogen species (Figure 2). After exposure of the probe to $ONOO^-$, the fluorescence signal changes could reach saturation within 10 min. As Figure 2 displayed, NO, H_2O_2, *tert*-butyl hydroperoxide (*t*-BuOOH), cumene hydroperoxide (CuOOH), and hypochlorite (ClO^-) triggered limited fluorescence responses within 30 min of the reaction. However, the fluorescence intensity increase was far weaker than that caused by $ONOO^-$. Next, we

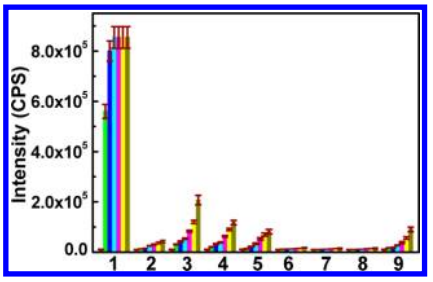

Figure 2. Time-dependent fluorescence response of 10 μM Cy-NTe to $ONOO^-$ and other biologically relevant reactive oxygen and nitrogen species. Bars represent fluorescence intensity at 820 nm during 0, 5, 10, 15, 20, 25, and 30 min after addition of various compounds. 1, $ONOO^-$ (10 μM); 2, NO (300 μM); 3, H_2O_2 (200 μM); 4, *tert*-butyl hydroperoxide (*t*-BuOOH, 250 μM); 5, cumene hydroperoxide (CuOOH, 300 μM); 6, methyl linoleate hydroperoxide (MeLOOH, 400 μM); 7, $^{\bullet}OH$ (200 μM); 8, $O_2^{\cdot-}$ (200 μM); **9**, ClO^- (200 μM). All data were acquired in 50 mM PBS (acetonitrile 10% v/v) at pH 7.4 (λ_{ex} = 793 nm, λ_{em} = 820 nm).

chose the mouse macrophage cell line RAW264.7 as a bioassay model to assess the specific nature of Cy-NTe toward $ONOO^-$ in cells. The test results were exhibited in Figure 3. Macrophage cells were treated with the following inducers, and then loaded with 1 μM Cy-NTe for 15 min, then washed the cells three times with RPMI-1640 before imaging. A high amount of intracellular peroxynitrite can be produced by inducible nitric

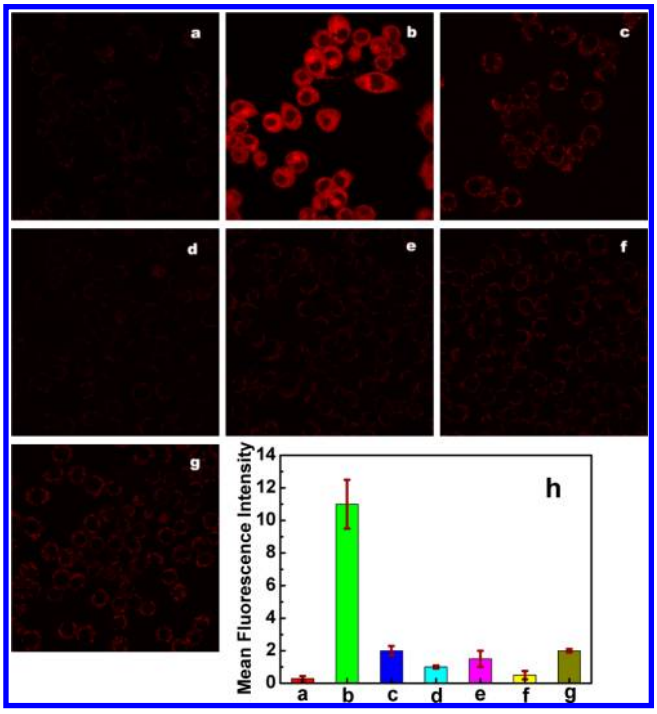

Figure 3. Fluorescence confocal microscopic images of RAW264.7 cells exposed to oxidative stress. Macrophage cells were treated with various inducers and then loaded with 1 μM Cy-NTe for 15 min (a) control. (b) LPS (1 μg/mL) and IFN-γ (50 ng/mL) for 4 h then PMA (10 nM) for 0.5 h. (c) AG (1 mM), LPS (1 μg/mL), and IFN-γ (50 ng/mL) for 4 h then PMA (10 nM) for 0.5 h. (d) PMA (10 nM) for 0.5 h. (e) Cells treated with 200 μM paraquat for 8 h. (f) The image after the administration of 50 μM NOC-5 for 3 min, (g) cells treated with 100 μM NaClO for 0.5 h. (h) Graph showing quantification of mean fluorescence intensity in a–g correspondingly. Scale bar = 20 μm.

dx.doi.org/10.1021/ja401360a | J. Am. Chem. Soc. 2013, 135, 7674–7680

oxide synthase 2 (NOS2) by bacterial products such as interferon-gamma (IFN-γ) and lipopolysaccharide (LPS).[23] Macrophages are additionally stimulated with phorbol 12-myristate 13-acetate (PMA) to provide an overproduction of superoxide during the peroxynitrite formation. The inducer, PMA, can also produce hydroxyl radical.[24] Qaraquat can trigger elevations in intracellular H_2O_2 through disruption of the mitochondrial electron transport chain.[25] NO is generated in form of 3-(aminopropyl)-1-hydroxy-3-isopropyl-2-oxo-1-triazene (NOC-5).[26] The hypochlorite (ClO^-) is directly from the sodium hypochlorite. There was almost no fluorescence in the absence ofstimulant (part a of Figure 3). However, strong fluorescence appeared after treatment with lipopolysaccharide (LPS 1 μg/mL) and interferon-γ (IFN-γ 50 ng/mL) for 4 h followed by additional stimulation with phorbol 12-myristate 13-acetate (PMA, 10 nM) for 0.5 h (part b of Figure 3). Whereas the cells were pretreated with aminoguanidine (AG), an inhibitor of nitric oxide synthase, much weaker fluorescence was detected in stimulated cells (part c of Figure 3). The hydroxyl radical (·OH) was produced by incubated cells with (PMA, 10 nM) for 0.5 h, and there was no fluorescence observed in part d of Figure 3. RAW264.7 cells were incubated with 200 μM paraquat for 8 h (part e of Figure 3). Together with RAW264.7 cells loaded with 50 μM NOC-5 for 3 min and 100 μM NaClO for 30 min also showed faint fluorescence (parts f and g of Figure 3). Part h of Figure 3 showed quantification of mean fluorescence intensity of each condition shown in parts a–g of Figure 3. Taken together, these selectivity assays demonstrate that the chemoselective oxidation of Cy-NTe can be used for fluorescence selective detection of $ONOO^-$ under simulated physiological conditions and in cells.

Detection of Mitochondrial Peroxynitrite in Macrophage Cells. Mitochondria are the cellular power plants. They are also involved in signaling, cellular differentiation, cell death, as well as the control of the cell cycle and cell growth.[27] Endogenous peroxynitrite are produced via the enzymatic activity of inducible nitric oxide synthase 2 (NOS2) and NADPH oxidase. NOS2 is expressed primarily in macrophages after induced by interferon-gamma (IFN-γ) and lipopolysaccharide (LPS). Additionally, mitochondrial electron leak is a main pathway to produce superoxide anion via NADPH oxidase. Therefore, mitochondrial respiration is a major source of peroxynitrite in macrophage cells.[1,9] We next assessed whether our probe Cy-NTe could respond to the mitochondrial peroxynitrite in living cells. Our probe Cy-NTe can exhibit a significant ability to target mitochondria because of the ammonium cation in cyanine fluorophore.[28] Co-localization can describe the existence of two or more molecular dyes in precisely the same space. Now we employed the colocalization method to confirm Cy-NTe sublocated in mitochondria. Co-localization experiments were performed by costaining RAW264.7 cells with rhodamine 123, a mitochondria tracker.[29] RAW264.7 cells were treated with LPS (1 μg/mL) and interferon-γ (IFN-γ 50 ng/mL) for 4 h followed by additional stimulation with phorbol 12-myristate 13-acetate (PMA, 10 nM) for 0.5 h. After washing with RPMI-1640, cells were loaded with 1 μM Cy-NTe and 5 μg/mL rhodamine 123 for 15 min. The image in part a of Figure 4 merged well with the image of staining with rhodamine 123 (part b of Figure 4), indicating the peroxynitrite oxidized probe Cy-NTeO could specifically localize in mitochondria. The intensity profiles of the linear regions of interest across RAW264.7 cells costained with Cy-NTeO and rhodamine 123 (red arrow in part c of Figure 4) are varying in close synchrony (part f of Figure 4). The Pearson's coefficient Rr = 0.94 and the Manders' coefficients m_1 = 0.99, m_2 = 0.98 were evaluated using Image-Pro Plus software. We also employed this software to carry a color intensity correlation analysis of parts a and b of Figure 4. We plotted the intensity of stain Cy-NTeO against that of rhodamine 123 for each pixel to assess the intensity distribution of the two colocalization dyes. The dependent staining in parts a and b of Figure 4 resulted in highly correlated plots (parts d and e of Figure 4).[30] All of these results made our probe a strong candidate for real-time imaging mitochondrial redox status changes caused by $ONOO^-$. In addition, to prove whether Cy-NTe had toxicity to cells, the MTT assay was performed. The result showed IC50 was 160 μM. It was demonstrated that the cytotoxicity of Cy-NTe was low under experimental conditions.

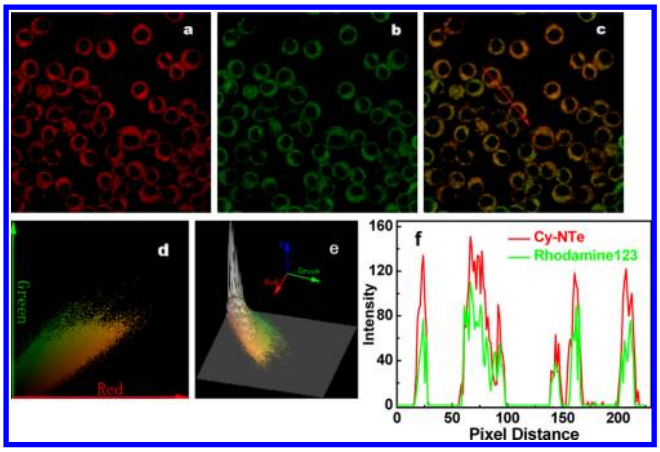

Figure 4. Cy-NTe and rhodamine 123 dye colocalization at mitochondria in RAW264.7 cells. Cells treated with LPS (1 μg/mL) and IFN-γ (50 ng/mL) for 4 h and then with PMA (10 nM) for 0.5 h, then cells were washed with RPMI-1640. The cells were loaded with 1 μM Cy-NTe (a), and 5 μg/mL rhodamine 123 (b) for 15 min. Fluorescence confocal microscopic images constructed from 790 to 860 nm for (a) and from 500 to 600 nm for (b) fluorescence collection windows, λ_{ex} = 780 and 488 nm, respectively. (c) Merged red channel (a) and green channel (b). (d) Displayed the colocalization areas of the red and green channels selected. (e) Co-localization plot of (a) and (b), z axis represents the frequency that color pair exists in (c), y and x axis represent the intensity of each pixel in (d). (f) Intensity profile of regions of interest (red arrow in (c) across RAW264.7 cells.

Investigation of the Reversibility of the Probe in Solution and in Cells. Next, we discussed the reversibility of the reaction between Cy-NTeO and GSH in solution and in cells. Considering the complex and diverse antioxidants contained in cells, an additional important work of the probe was carried out to determine which antioxidant could trigger the fluorescent switch off efficaciously. As shown in part a of Figure 5, Cy-NTeO exhibited a quick decrease in fluorescence intensity upon reaction with GSH and cysteine. The fluorescence recovery rate could be up to 97% within 5 min. Other protein thoils including thioedoxinand and metallothionein induced limited fluorescent response, whereas the responses toward other antioxidants, such as vitamin C, vitamin E, uric acid, and histamine were negligible during the 30 min experiment (part a of Figure 5). Because the concentration of mitochondrial GSH was far higher than that of mitochondrial cysteine, protein thoils, and other endogenous antioxidants,[9,31] we considered that the fluorescence signal could be regarded as

dx.doi.org/10.1021/ja401360a | J. Am. Chem. Soc. 2013, 135, 7674–7680

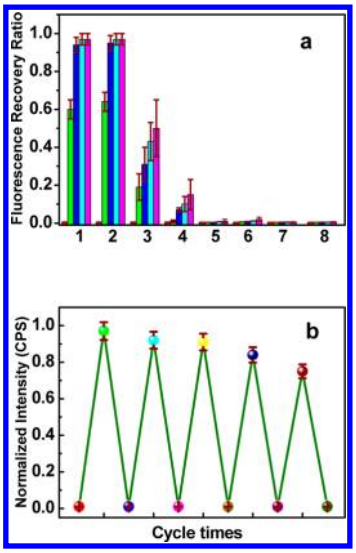

Figure 5. (a) Fluorescence recovery ratio of Cy-NTeO (10 μM) with the addition of different biological reductants during 30 min. Bars represent fluorescence intensity at 0, 3, 5, 20, and 30 min. All reductants at 500 μM. 1, L-cysteine; 2, glutathione; 3, thioedoxin; 4, metallothionein; 5, vitamin C; 6, vitamin E; 7, uric acid; 8, histamine. Fluorescence recovery ratio = $(F - F_0)/F$; where F is the fluorescence intensity of Cy-NTeO (10 μM), F_0 is the fluorescence intensity of the probe after adding different biological reductants. (b) Normalized fluorescence responses of Cy-NTe (10 μM) to redox cycles. Cy-NTe was oxidized by 1 equiv of added $ONOO^-$. Ten minutes later, the solution was treated with 2 equiv of GSH. When fluorescence returned to the starting levels, another 1 equiv of $ONOO^-$ was added to the mixture. The redox cycle was repeated 5 times. $ONOO^-$ is from a peroxynitrite donor, 3-morpholinosydnonimine (SIN-1). All data were acquired in 50 mM PBS (acetonitrile 10% v/v) at pH 7.4 (λ_{ex}= 793 nm, λ_{em} = 820 nm).

a response of Cy-NTeO to mitochondrial GSH when the probe is used in living cells. Part b of Figure 5 showed that the reversible oxidation−reduction cycle could be repeated at least 5 times with only a modest fluorescence decrement (25% of Cy-NTeO was bleached during the process). Taken together, Cy-NTe was suitable for mitochondrial peroxynitrite reversible monitoring in living cells.

Because the probe Cy-NTe exhibited high redox sensitivity, selectivity, and reversibility, we next verified whether it could monitor $ONOO^-$ reversible redox cycles in the mitochondria of living cells using confocal fluorescence microscopy. The experimental results were shown in Figure 6. Macrophage cells were loaded with 1 μM Cy-NTe for 15 min, and then washed the cells three times with RPMI-1640. There was almost no fluorescence (part a of Figure 6). Strong fluorescence appeared after treatment with LPS (1 μg/mL) and interferon-γ (IFN-γ 50 ng/mL) for 4 h followed by additional stimulation with phorbol 12-myristate 13-acetate (PMA, 10 nM) for 0.5 h (part b of Figure 6), whereas the cells were pretreated with aminoguanidine (AG), an inhibitor of nitric oxide synthase, and the reactive oxygen species scavenger glutathione S-transferase (GST, EC 2.5.1.18; 250 units/mL) much weaker fluorescence was detected (part c of Figure 6). Addition of an aliquot of 100 μM 3-morpholinosydnonimine (SIN-1, a common peroxynitrite donor) oxidant resulted in another burst of oxidative stress and an increase in intracellular fluorescence (part d of Figure 6). The same cells were washed with RPMI-1640, then added L-cysteine (1 mM) and GST (250

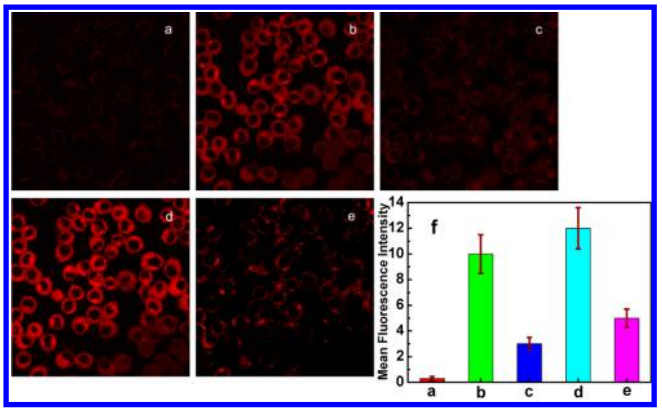

Figure 6. Fluorescence confocal microscopic images of RAW264.7 cells loaded with 1 μM Cy-NTe and exposed to redox cycles between peroxynitrite and GSH. (a) Cells were incubated under 37 °C for 5 min in RPMI-1640 containing 1 μM Cy-NTe, then washed with RPMI-1640, and placed in fresh RPMI-1640. (b) Dye-loaded cells treated with LPS (1 μg/mL) and IFN-γ (50 ng/mL) for 4 h then PMA (10 nM) for 0.5 h. (c) Cells were washed with RPMI-1640, added AG (1 mM) and GST (250 units/mL), then incubated in the fresh complete medium (RPMI-1640 + 20% FBS) for 15 min (d) cells were washed with RPMI-1640 and placed in fresh RPMI-1640, then treated with 100 μM SIN-1 for 20 min (e) cells were washed with RPMI-1640, added L-cysteine (1 mM) and GST (250 units/mL), then incubated in the fresh complete medium (RPMI-1640 + 20% FBS) for 15 min (f) quantification of mean fluorescence intensity in (a−e) correspondingly. Scale bar = 20 μm.

units/mL) in the fresh complete medium (RPMI-1640 + 20% FBS) for the further culture 15 min, the image exhibited a large fluorescence decrement (part e of Figure 6). Part f of Figure 6 showed quantification of mean fluorescence intensity of each condition shown in parts a−e of Figure 6. Taken together, these results indicate that Cy-NTe allows the reversible detection of the mitochondrial $ONOO^-$ reversible redox cycles with high sensitivity and reversibility.

Visualization of $ONOO^-$ Redox Reversibility in Living Mice. Cy-NTe will be favorable for bioimaging applications in living animals because NIR light can penetrate tissue deeply and minimize the interference form background autofluorescence. We next sought to apply Cy-NTe to fluorescent imaging of $ONOO^-$ redox cycles in vivo. We utilized BALB/c mice as biological models. Cy-NTe (1 μM, 50 μL in 1:9 DMSO/saline v/v) was injected into intraperitoneal (i.p.) cavity of BALB/c mice, and the fluorescent signal produced by our probe was imaged using a CCD camera after 30 min (part b of Figure 7). Another mice in part a of Figure 7 was injected with Cy-NTe (1 μM, 50 μL in 1:9 DMSO/saline v/v) and L-cysteine (1 mM, 100 μL in saline). As shown in part f of Figure 7, the data suggest that Cy-NTe may be sensitive enough to detect basal levels of $ONOO^-$ that are endogenously produced without stimulating $ONOO^-$ production highlighting the potential utility of Cy-NTe for $ONOO^-$ detection in vivo. Mice in part c of Figure 7 were injected i.p. with LPS (10 μg/mL) and IFN-γ (200 ng/mL) for 4 h and then with PMA (100 nM) for 0.5 h and next loaded with 1 μM Cy-NTe for 30 min. We were pleased to observe that the drug-treated animals give a significantly increased fluorescent signal compared to the control animals in part a of Figure 7. Mice in part d of Figure 7 were treated as part c of Figure 7 described continued to inject into i.p. with AG (1 mM, 100 μL in 1:9 DMSO/saline v/v), GST (250 units/mL, 300 μL in saline), and L-cysteine (1

dx.doi.org/10.1021/ja401360a | J. Am. Chem. Soc. 2013, 135, 7674−7680

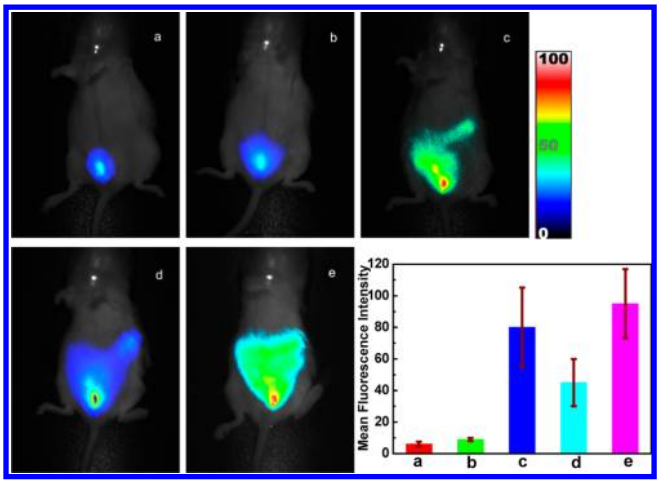

Figure 7. Imaging of redox cycles between peroxynitrite and GSH in peritoneal cavity of the mice BALB/c. (a) Cy-NTe (1 μM, 50 μL in 1:9 DMSO/saline v/v) and L-cysteine (1 mM, 100 μL in saline) were injected in the i.p. cavity. (b) Mice injected i.p. with Cy-NTe (1 μM, 50 μL in 1:9 DMSO/saline v/v). (c) Mice injected i.p. with LPS (10 μg/mL) and IFN-γ (200 ng/mL) for 4 h and then with PMA (100 nM) for 0.5 h, then loaded with 1 μM Cy-NTe for 30 min (d) Mice treated as (c) described, then injected i.p. with AG (1 mM, 100 μL in 1:9 DMSO/saline v/v), GST (250 units/mL, 300 μL in saline), and L-cysteine (1 mM, 200 μL in saline). (e) Mice treated as d) described, then injected i.p. with SIN-1 (1 mM, 1 mL in saline) for 20 min (f) Quantification of total photon flux from each mouse (a–e). The total number of photons from the entire peritoneal cavity of the mice (a–e) was integrated. Images constructed from 790 to 860 nm fluorescence collection window, λ_{ex} = 735 nm.

mM, 200 μL in saline) for 30 min, the mice exhibited a large fluorescence decrement compared to the animals in part c of Figure 7. The final group mice were first treated as part d of Figure 7 described then injected i.p. with SIN-1 (1 mM, 1 mL in saline) for 20 min. The mice exhibited a significantly higher fluorescence increase. Part f of Figure 7 showed quantification of mean fluorescence intensity of each condition shown in parts a–e of Figure 7. These results establish that Cy-NTe is sensitive enough to visualize the redox cycles between peroxynitrite and GSH in living animals indicating the advantage of the new reversible near-infrared fluorescent probe Cy-NTe.

CONCLUSIONS

In summary, we have presented a new reversible near-infrared fluorescent probe Cy-NTe to evaluate the $ONOO^-$/GSH redox status in cells and in vivo. We design the probe through the synthesis of telluroenzyme, a GPx-like analogue that interacts with $ONOO^-$/GSH to trigger the fluorescent response cycles. This mitochondria-targeted fluorescent probe shows a turn on fluorescence response to endogenous $ONOO^-$ that is selective over a variety of reactive nitrogen and oxygen species and can be reduced by intracellular GSH. This small-molecule imaging probe is able to work well in the body of living mice. The probe is successfully applied to real-time imaging the changes of $ONOO^-$/GSH redox homeostasis in cells and mice. Our data confirm that Cy-NTe is a viable fluorescent probe for the reversible detection of fluctuations in $ONOO^-$ produced in cells and living animals.

ASSOCIATED CONTENT

Supporting Information

Experimental conditions, supplementary methods for chemical synthesis and characterization of compounds, supplementary experiments and data. This material is available free of charge via the Internet at http://pubs.acs.org.

AUTHOR INFORMATION

Corresponding Author

*E-mail: klhan@dicp.ac.cn.

Notes

The authors declare no competing financial interest.

ACKNOWLEDGMENTS

This work was supported by NSFC Nos. 21273234, 21203192, and 2013CB834604.

REFERENCES

(1) (a) Ferrer-Sueta, G.; Radi, R. *ACS Chem. Biol.* **2009**, *4*, 161. (b) Pacher, P.; Beckman, J. S.; Liaudet, L. *Physiol. Rev.* **2007**, *87*, 315.

(2) (a) Surmeli, N. B.; Litterman, N. K.; Miller, A.-F.; Groves, J. T. *J. Am. Chem. Soc.* **2010**, *132*, 17174. (b) Liaudet, L.; Vassalli, G.; Pacher, P.; Biosci, F. *Free Radical Biol. Med.* **2009**, *14*, 4809. (c) Shiddipui, M. R.; Komarava, Y. A.; Vogel, S. M.; Gao, X.; Bonini, M. G.; Rajasingh, J.; Zhao, Y.; Brokovych, V.; Malik, A. B. *J. Cell Biol.* **2011**, *193*, 841. (d) Kawasaki, H.; Ikeda, K.; Shigenaga, A.; Baba, T.; Takamori, K.; Ogawa, H.; Yamakura, F. *Free Radical Biol. Med.* **2011**, *50*, 419. (e) Sawa, T.; Zaki, M. H.; Okamoto, T.; Akuta, T.; Tokutomi, Y.; Kim-Mitsuyama, S.; Ihara, H.; Kobayashi, A.; Yamamoto, M.; Fujii, S.; Arimoto, H.; Akaike, T. *Nat. Chem. Biol.* **2007**, *3*, 727. (f) Khoo, N. K. H.; Freeman, B. A. *Curr. Opin. Pharmacol.* **2010**, *10*, 179.

(3) (a) Fraszczak, J.; Trad, M.; Janikashvili, N.; Cathelin, D.; Lakomy, D.; Granci, V.; Morizot, A.; Audila, S.; Micheau, O.; Lagrost, L.; Katsanis, E.; Solary, E.; Larmonier, N.; Bonnotte, B. *J. Immunol.* **2010**, *184*, 1876. (b) Ieda, N.; Nakagawa, H.; Peng, T.; Yang, D.; Suzuki, T.; Miyata, N. *J. Am. Chem. Soc.* **2012**, *134*, 2563. (c) Gryglewski, R. J.; Palmer, R. M.; Moncada, S. *Nature* **1986**, *320*, 454. (d) Peluffo, G.; Alvarez, M. N.; Naviliat, M.; Cayota, A. *Free Radical Biol. Med.* **2001**, *30*, 463.

(4) (a) Alvarez, M. N.; Piacenza, L.; Irigoin, F.; Peluffo, G.; Radi, R. *Biochem. Biophys.* **2004**, *432*, 222. (b) St John, G.; Brot, N.; Ruan, J.; Erdjument-Bromage, H.; Tempst, P.; Weissbach, H.; Nathan, C. *Proc. Natl. Acad. Sci. U. S. A.* **2001**, *98*, 9901. (c) Darrah, P. A.; Hondalus, M. K.; Chen, Q.; Ischiropoulos, H.; Mosser, D. M. *Infect. Immun.* **2000**, *68*, 3587.

(5) (a) Nalwaya, N.; Deen, W. M. *Chem. Res. Toxicol.* **2005**, *18*, 486. (b) Quijano, C.; Romero, N.; Radi, R. *Free Radical Biol. Med.* **2005**, *39*, 728.

(6) (a) Chen, X.; Zhou, Y.; Peng, X.; Yoon, J. *Chem. Soc. Rev.* **2010**, *39*, 2120. (b) Wang, R.; Yu, C.; Yu, F.; Chen, L. *Trends Anal. Chem.* **2010**, *29*, 1004. (c) Chen, X.; Tian, X.; Shin, I.; Yoon, J. *Chem. Soc. Rev.* **2011**, *40*, 4783. (d) Chan, J.; Dodani, S. C.; Chang, C. J. *Nat. Chem.* **2012**, *4*, 973. (e) Yang, Y.; Zhao, Q.; Feng, W.; Li, F. *Chem. Rev.* **2013**, *113*, 192. (f) Shi, W.; Ma, H. *Chem. Commun.* **2012**, *48*, 8732. (g) Dsouza, R. N.; Pischel, U.; Nau, W. M. *Chem. Rev.* **2011**, *111*, 7941. (h) Duke, R. M.; Veale, E. B.; Pfeffer, F. M.; Kruger, P. E.; Gunnlaugsson, T. *Chem. Soc. Rev.* **2010**, *39*, 3936. (i) Chen, X.; Pradhan, T.; Wang, F.; Kim, J. S.; Yoon, J. *Chem. Rev.* **2012**, *112*, 1910.

(7) (a) Wang, R.; Chen, L.; Liu, P.; Zhang, Q.; Wang, Y. *Chemistry* **2012**, *18*, 11343. (b) Yu, F.; Li, P.; Song, P.; Wang, B.; Zhao, J.; Han, K. *Chem. Commun.* **2012**, *48*, 4980. (c) Niu, L.; Guan, Y.; Chen, Y.; Wu, L.; Tung, C.; Yang, Q. *J. Am. Chem. Soc.* **2012**, *134*, 18928. (d) Lee, M. H.; Han, H.; Lee, J. H.; Choi, H. G.; Kang, C.; Kim, J. S. *J. Am. Chem. Soc.* **2012**, *134*, 17314.

(8) Morgan, B.; Ezerina, D.; Amoako, T. N.; Riemer, J.; Seedorf, M.; Dick, T. P. *Nat. Chem. Biol.* **2012**, *9*, 1142.

(9) (a) Radi, R.; Cassina, A.; Hodara, R.; Quijano, C.; Castro, L. *Free Radical Biol. Med.* **2002**, *33*, 1451. (b) Novo, E.; Parola, M. *Fibrog. Tissue Repair* **2008**, *1*, 5.
(10) Lim, C. S.; Masanta, G.; Kim, H. J.; Han, J. H.; Kim, H. M.; Cho, B. R. *J. Am. Chem. Soc.* **2011**, *133*, 11132.
(11) (a) Ueno, T.; Urano, Y.; Setsukinai, K.; Takakusa, H.; Kojima, H.; Kikuchi, K.; Ohkubo, K.; Fukuzumi, S.; Nagano, T. *J. Am. Chem. Soc.* **2004**, *126*, 14079. (b) Ueno, T.; Urano, Y.; Kojima, H.; Nagano, T. *J. Am. Chem. Soc.* **2006**, *128*, 10640. (c) Yang, D.; Wang, H.; Sun, Z.; Chung, N.-W.; Shen, J. *J. Am. Chem. Soc.* **2006**, *128*, 6004. (d) Sun, Z.; Wang, H.; Liu, F.; Chen, Y.; Tam, P. K. H.; Yang, D. *Org. Lett.* **2009**, *11*, 1887. (e) Hempel, S. L.; Buettner, G. R.; O'Malley, Y. Q.; Wessels, D. A.; Flaherty, D. M. *Free Radical Biol. Med.* **1999**, *27*, 146. (f) Miyasaka, N.; Hirata, Y. *Life Sci.* **1997**, *61*, 2073. (g) Oushiki, D.; Kojima, H.; Terai, T.; Arita, M.; Hanaoka, K.; Urano, Y.; Nagano, T. *J. Am. Chem. Soc.* **2010**, *132*, 2795. (h) Peng, T.; Yang, D. *Org. Lett.* **2010**, *12*, 4932. (i) Zielonka, J.; Sikora, A.; Joseph, J.; Kalyanaraman, B. *J. Biol. Chem.* **2010**, *285*, 14210. (j) Yang, X. F.; Guo, X. Q.; Zhao, Y. B. *Talanta* **2002**, *57*, 883. (k) Setsukinai, K.; Urano, Y.; Kakinuma, K.; Majima, H. J.; Nagano, T. *J. Biol. Chem.* **2003**, *278*, 3170. (l) Song, C.; Ye, Z.; Wang, G.; Yuan, J.; Guan, Y. *Chem.—Eur. J.* **2010**, *16*, 6464. (m) Zhang, Q.; Zhu, Z.; Zheng, Y.; Cheng, J.; Zhang, N.; Long, Y, T.; Zheng, J.; Qian, X.; Yang, Y. *J. Am. Chem. Soc.* **2012**, *134*, 18479. (n) Wang, B.; Yu, F.; Li, P.; Sun, X.; Han, K. *Dyes Pigm.* **2013**, *96*, 383. (o) Yu, F.; Song, P.; Li, P.; Wang, B.; Han, K. *Analyst* **2012**, *137*, 3740.
(12) Miller, E. W.; Bian, S. X.; Chang, C. J. *J. Am. Chem. Soc.* **2007**, *129*, 3458.
(13) (a) Yamada, Y.; Tomiyama, Y.; Morita, A.; Ikekita, M.; Aoki, S. *ChemBioChem* **2008**, *9*, 853. (b) Lee, K.; Dzubeck, V.; Latshaw, L.; Schneider, J. P. *J. Am. Chem. Soc.* **2004**, *126*, 13616. (c) Hilberbrand, S. A.; Lim, M. H.; Lippard, S. T. *J. Am. Chem. Soc.* **2004**, *126*, 4972. (d) Koide, Y.; Kawaguchi, M.; Urano, Y.; Hanaoka, K.; Komatsu, T.; Abo, M.; Terai, T.; Nagano, T. *Chem. Commun.* **2012**, *48*, 3091. (e) Reddie, K. G.; Humphries, W. H.; Bain, C. P.; Payne, C. K.; Kemp, M. L.; Murthy, N. *Org. Lett.* **2012**, *14*, 680. (f) Takahashi, S.; Piao, W.; Matsumura, Y.; Komatsu, T.; Ueno, T.; Terai, T.; Kamachi, T.; Kohno, M.; Nagano, T.; Hanaoka, K. *J. Am. Chem. Soc.* **2012**, *134*, 19588. (g) Yu, F.; Song, P.; Li, P.; Wang, B.; Han, K. *Chem. Commun.* **2012**, *48*, 7735.
(14) (a) Yu, F.; Li, P.; Zhao, G.; Chu, T.; Han, K. *J. Am. Chem. Soc.* **2011**, *133*, 11030. (b) Wang, B.; Li, P.; Yu, F.; Song, P.; Sun, X.; Yang, S.; Lou, Z.; Han, K. *Chem. Commun.* **2013**, *49*, 1014. (c) Lou, Z.; Li, P.; Sun, X.; Yang, S.; Wang, B.; Han, K. *Chem. Commun.* **2013**, *49*, 391. (d) Lou, Z.; Li, P.; Pan, Q.; Han, K. *Chem. Commun.* **2013**, *49*, 2445.
(15) Bhabak, K. P.; Mugesh, G. *Acc. Chem. Res.* **2010**, *43*, 1408.
(16) (a) Lalla, A. B.; Mandy, D.; Vincent, J.; Claus, J. *Org. Biomol. Chem.* **2010**, *8*, 4203. (b) Nogueira, C. W.; Zeni, G.; Rocha, J. B. *Chem. Rev.* **2004**, *104*, 6255.
(17) Sarma, B. K.; Manna, D.; Minoura, M.; Mugesh, G. *J. Am. Chem. Soc.* **2010**, *132*, 5364.
(18) (a) Frangioni, J. *Curr. Opin. Chem. Biol.* **2003**, *7*, 626. (b) Hirayama, T.; Van de Bittner, G. C.; Gray, L. W.; Lutsenko, S.; Chang, C. J. *Proc. Natl. Acad. Sci. U. S. A.* **2012**, *109*, 2228. (c) Yuan, L.; Lin, W.; Zheng, K.; He, L.; Huang, W. *Chem. Soc. Rev.* **2012**, *42*, 622.
(19) Sasaki, E.; Kojima, H.; Nishimatsu, H.; Urano, Y.; Kikuchi, K.; Hirata, Y.; Nagano, T. *J. Am. Chem. Soc.* **2005**, *127*, 3684.
(20) Aso, Y.; Yamashita, H.; Otsubo, T.; Ogura, F. *J. Org. Chem.* **1989**, *54*, 5627.
(21) Kundu, D.; Ahammed, S.; Ranu, B. C. *Green Chem.* **2012**, *14*, 2024.
(22) Samanta, A.; Maiti, K. K.; Soh, K. S.; Liao, X.; Vendrell, M.; Dinish, U. S.; Yun, S. W.; Bhuvaneswari, R.; Kim, H.; Rautela, S.; Chung, J.; Olivo, M.; Chang, Y. T. *Angew. Chem., Int. Ed.* **2011**, *50*, 6089.
(23) (a) Muijsers, R. B; van Den Worm, E.; Folkerts, G.; Beukelman, C. J.; Koster, A. S.; Postma, D. S.; Nijkamp, F. P. *Br. J. Pharmacol.* **2000**, *130*, 932. (b) Salonen, T.; Sareila, O.; Jalonen, U.; Kankaanranta, H.; Tuominen, R.; Moilanen, E. *Br. J. Pharmacol.* **2006**, *147*, 790.
(24) Hecker, E.; Schmidt, R. *Prog. Chem. Org. Nat. Prod.* **1974**, *31*, 377.
(25) Van de Bittner, G. C.; Dubikovskaya, E. A.; Bertozzi, C. R.; Chang, C. J. *Proc. Natl. Acad. Sci. U. S. A.* **2010**, *107*, 21316.
(26) Maeda, H.; Yamamoto, K.; Nomura, Y.; Kohno, I.; Hafsi, L.; Ueda, N.; Yoshida, S.; Fukuda, M.; Fukuyasu, Y.; Yamauchi, Y.; Itoh, N. *J. Am. Chem. Soc.* **2005**, *127*, 68.
(27) Green, D. R.; Galluzzi, L.; Kroemer, G. *Science* **2011**, *333*, 1109.
(28) Johnson, L. V.; Walsh, M. L.; Bockus, B. J.; Chen, L. J. *Cell Biol.* **1981**, *88*, 526.
(29) Johnson, L. V.; Walsh, M. L.; Chen, L. *Proc. Natl. Acad. Sci. U. S. A.* **1980**, *77*, 990.
(30) Wu, Y.; Zinchuk, V.; Grossenbacher-Zinchuk, O.; Stefani, E. *Interdiscip. Sci.* **2012**, *4*, 27.
(31) Karp, D. R.; Shimooku, K.; Lipsky, P. E. *J. Biol. Chem.* **2001**, *276*, 3798.